

# Thermal Characterization of Three-Component Blends for Hot-Melt Adhesives

E. G. FERNANDES, A. LOMBARDI, R. SOLARO, E. CHIellini

Department of Chemistry and Industrial Chemistry, University of Pisa, via Risorgimento 35, 56126 Pisa, Italy

Received 10 October 1999; accepted 10 August 2000

**ABSTRACT:** Traditional solvent-based adhesives used in the footwear industry have been demonstrated as harmful to the workers' health and environment. Solvent-free three-component adhesives (hot-melt adhesives or HMAs) for various applications including the leather and footwear industry are becoming more and more attractive. Thus, the formulation of a three-component HMA was realized in this study. Thermogravimetry, differential scanning calorimetry, and the apparent strength of the adhesive bond were used to investigate the relationship between their properties and the polymer/wax/resin compositions. The thermal stability of HMA formulations was determined and compared with thermal traces based on an additive weight computation of the single components' thermal profiles. All HMA formulations showed a direct relationship between the glass-transition temperature and the apparent adhesive shear strength at the leather-rubber interface. © 2001 John Wiley & Sons, Inc. *J Appl Polym Sci* 80: 2889–2901, 2001

**Key words:** hot-melt adhesive; polymer blends; thermal analysis; leather; shear strength

## INTRODUCTION

In general, footwear adhesives are formulated with volatile organic solvents that are known to cause safety problems for the environment and health.<sup>1,2</sup> Some of the most commonly used ones are toluene, methyl ethyl ketone, and chloroform. Nowadays there is a fast growing interest in solvent-free adhesives (hot-melt adhesives or HMAs) for specific applications with a major share of them being in the footwear industry.

The most common polymers used in HMAs do not exhibit the performance characteristics required for an end product. A variety of materi-

als must be added to the polymer matrix to attain the desired HMA properties. Among them, two components exhibit an important role in the adhesive application: a tackifier resin and wax. The tackifier is responsible for the tackiness and wetting, while wax is added to decrease the formulation viscosity and accelerate solidification during cooling.<sup>3–6</sup> The compatibility of the tackifier resin with the matrix polymer has a direct relationship with the HMA performance. Formulations containing styrene-butadiene block copolymers (SBS) as the main component were studied by Galán et al.<sup>7</sup> Their results showed that high adhesive performance can be obtained from tackifiers that have good compatibilities with both the end and midblock of the SBS copolymer or at least with the polybutadiene midblock. Besides, the tackifier concentrations do not have to be higher than 45–50%. Another study of HMAs based on an SBS

Correspondence to: E. Chiellini (chlmeo@cci.unipi.it).

Contract grant sponsor: Ministry, University of Pisa, PRIN 98 Sintesi di Materiali Polimerici per Applicazioni non Convenzionali.

*Journal of Applied Polymer Science*, Vol. 80, 2889–2901 (2001)  
© 2001 John Wiley & Sons, Inc.

copolymer was carried out by Sung and coworkers.<sup>8</sup> The results they reported nicely complement the former findings of Galán et al.<sup>7</sup> From dynamic mechanical measurements and morphological observations they verified that the storage modulus ( $G'$ ) of the blend increased when the tackifier was compatible with the polystyrene end block or incompatible with the SBS copolymer. However, the highest peel strength was observed for the compatible blends. Moreover, when the tackifier was compatible with the polybutadiene midblock a considerable improvement in the adhesive properties was observed. Indeed, the blend with SBS not only showed a  $G'$  lower than that of SBS but also was characterized by good peel strength. Fujita et al. studied the effects of miscibility of several natural rubber–tackifier blends on probe tack and peel strength properties.<sup>9,10</sup> They found that miscible systems showed maximum probe tack values that were due to an increase of the glass-transition temperature ( $T_g$ ) with the tackifier concentration and a decrease in the apparent viscosity with consequent better wettability as a result of the blend homogeneity. In the peel strength, immiscible blends presented lower values than the miscible ones as detected in SBS adhesive formulations. HMAs based on an ethylene–vinyl acetate copolymer (EVA) thermoplastic were studied by Turreda and coworkers.<sup>11</sup> The evaluation of the relationship between the dynamic viscoelastic and adhesion strength properties of the compatible EVA–tackifier resin blends constituted the focal point of their investigation. These properties were verified over a wide range of test rates, stresses, and temperatures. The shear, tensile, and peel strength behavior of the blends were characterized by three regions corresponding to viscous, rubbery, and glassy adhesive responses. The shear and tensile strength master curves recorded for the blends with the increase of the tackifier resin shifted to the lower test rates.

Thermal analysis has been demonstrated to be an extremely suitable and widely used technique to determine the compatibility of blends.<sup>12,13</sup> However, little attention has been devoted to their degradation behavior.<sup>14</sup>

In the present work, three-component blends comprising polymer, tackifier, and wax were characterized by differential scanning calorimetry (DSC) and thermogravimetry (TG). The relation-

ship between the glass-transition temperature and the apparent strength of the adhesively bonded leather–rubber materials were investigated.

## EXPERIMENTAL

### Materials

Commercial Evatane® 28-05 [poly(ethylene-*co*-vinyl acetate), EVA, 27–29 wt % of vinyl acetate] and Lotader® AX 8920 [poly(ethylene-*co*-alkyl acrylate-*co*-glycidyl methacrylate), AX], both from Elf Atochem, were used as the base materials of the HMA formulations.

Two resins were used as tackifying agents: PK 500 (PK) terpene phenolic resin and ST 5040 (ST) terpenic resin from Hoechst and Schenectady Europe, respectively. The branched polyethylene (PE) wax PE 520 ( $d_{20} = 0.93 \text{ g/cm}^3$ , viscosity at  $140^\circ\text{C} = 650 \text{ mPa s}$ ) and Hostalub polar wax H12 ( $d_{20} = 0.95 \text{ g/cm}^3$ , acid value =  $18 \text{ mg KOH/g}$ , viscosity at  $140^\circ\text{C} = 350 \text{ mPa s}$ ), both from Hoechst, were used as wax components.

The compositions of the Evatane/resin/wax and Lotader/resin/wax blends are presented in Tables I and II, respectively. The wax concentration was fixed at 10 wt % in all cases.

Blends were prepared by thoroughly mixing the components in a beaker maintained at  $150\text{--}180^\circ\text{C}$  by a thermostated oil bath. The polymer was added first; then the wax and the resin were incorporated in the molten polymer in that order. The mixing time was between 30 and 60 min.

Blend sheets about 1 mm thick were prepared by compression molding at  $150\text{--}160^\circ\text{C}$  to test the adhesion between the leather and Vibram® rubber.

### Methods and Test Procedure

The TG and DSC analyses were performed with a Mettler TA 4000 System. A TG50/M3 thermobalance was used in the thermal stability determinations. Measurements were performed on samples of about 20 mg in a temperature range of  $25\text{--}600^\circ\text{C}$  at  $10^\circ\text{C min}^{-1}$  under a nitrogen flow of  $200 \text{ mL min}^{-1}$ . The DSC measurements were carried out with a DSC 30 cell. Samples of about 10 mg were heated, cooled, and heated again from

**Table I Formulation Characteristics of Blends Based on Evatane**

Sample	Blend Composition				Blending Temp. (°C)
	EVA (wt %)	Resin		Wax <sup>a</sup> Type	
		Type	(wt %)		
EVAH	90	—	—	H12	150
EVAPE	90	—	—	PE	150
EVA <sub>1</sub> STH	56	ST	44	—	160
EVA <sub>1</sub> PKH	56	PK	44	—	160
EVA <sub>1</sub> STPE	70	ST	20	H12	150
EVA <sub>2</sub> STH	50	ST	40	H12	160
EVA <sub>1</sub> STPE	70	ST	20	PE	160
EVA <sub>2</sub> STPE	50	ST	40	PE	160
EVA <sub>1</sub> PKH	70	PK	20	H12	180
EVA <sub>2</sub> PKH	50	PK	40	H12	180
EVA <sub>1</sub> PKPE	70	PK	20	PE	160
EVA <sub>2</sub> PKPE	50	PK	40	PE	170

EVA, Evatane polymer matrix; ST and PK, ST5040 and PK500 resins, respectively; H and PE, H12 and PE520 waxes, respectively.

<sup>a</sup> Concentration = 10 wt %.

–100 to 150°C at 10°C min<sup>-1</sup> under a nitrogen flow rate of 80 mL min<sup>-1</sup>.

Adhesion evaluation was carried out with an Instron material testing system (series 5565) following the ASTM D 3163-92 standard method.<sup>15</sup> The crosshead speed was set to 10 mm min<sup>-1</sup> due to the

flexibility characteristics of the samples. Test specimens were prepared in a mold as shown in Figure 1. An adhesive sheet (with a joint surface of about 5 cm<sup>2</sup>) was applied between the leather (25 × 80 × 3 mm) and rubber (25 × 80 × 4 mm) sheets by thermal compression molding at 150–160°C. Prior to

**Table II Formulation Characteristics of Blends Based on Lotader**

Sample	Blend Composition				Blending Temp. (°C)
	AX (wt %)	Resin		Wax <sup>a</sup> Type	
		Type	(wt %)		
AXH	90	—	—	H12	170
AXPE	90	—	—	PE	160
AXST	56	ST	44	—	160
AXPK	56	PK	44	—	180
AX <sub>1</sub> STH	70	ST	20	H12	160
AX <sub>2</sub> STH	50	ST	40	H12	160
AX <sub>1</sub> STPE	70	ST	20	PE	160
AX <sub>2</sub> STPE	50	ST	40	PE	160
AX <sub>1</sub> PKH	70	PK	20	H12	180
AX <sub>2</sub> PKH	50	PK	40	H12	180
AX <sub>1</sub> PKPE	70	PK	20	PE	180
AX <sub>2</sub> PKPE	50	PK	40	PE	180

AX, Lotader polymer matrix; ST and PK, ST5040 and PK500 resins, respectively; H and PE, H12 and PE520 waxes, respectively.

<sup>a</sup> Concentration = 10 wt %.

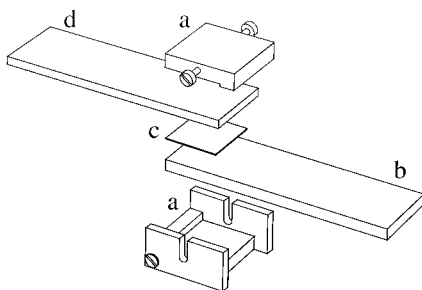


**Figure 1** A schematic representation of the mold used for the preparation of specimens for adhesion evaluation: (a) aluminum molds, (b) rubber ( $25 \times 80 \times 4$  mm), (c) adhesive sheet ( $22 \times 22 \times 1$  mm), and (d) leather ( $25 \times 80 \times 3$  mm).

the adhesion tests the rubber surface was roughened using grid emery paper and the leather surface was peeled with a cutter.

## RESULTS AND DISCUSSION

### TG Analysis

#### EVA Blends

Thermogravimetric traces of the EVA/resin/H12 (50/40/10 wt %) blend and its pure components are displayed in Figures 2 and 3. For comparison,

the calculated TG curve obtained by weighed addition of the thermogravimetric traces of the pure components is also reported.<sup>16</sup> Blends containing PE wax showed similar behavior.

Pure waxes and resins show only one weight loss step whereas pure EVA and EVA/resin/wax blends are characterized by two weight loss steps. The TG traces of binary EVA/wax blends (not shown) presented a profile similar to that of pure EVA with a slight difference in the first weight loss step, which was attributed to acetic acid loss from the vinyl acetate segment. The ST (Fig. 2) and PK (Fig. 3) represented the least stable component of the blends. Therefore, a decrease of blend stability could be expected as determined by the resin thermodecomposition if no specific interactions existed among the different components and/or among blend components and degradation products being formed (additive rule). This means that different reaction mechanisms may take place among all species present (macromolecules, macroradicals, small molecules and small radicals). These could either accelerate or refrain the blend degradation in respect to that observable for the corresponding pure components.

Apparently, experimental traces of EVA/ST/H12 blends indicated it to be slightly more stable at pyrolytic onset than would be expected from

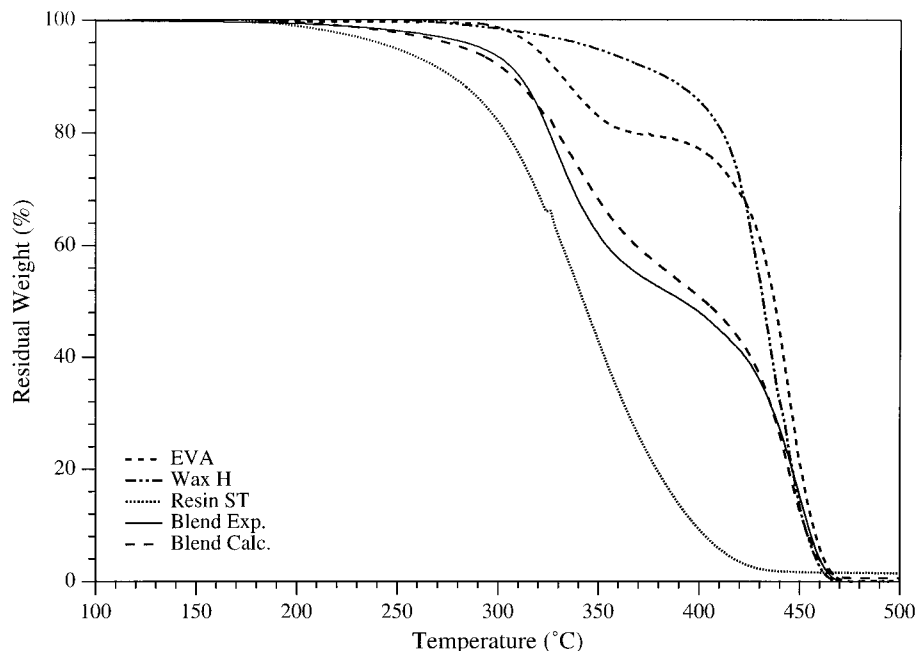


**Figure 2** Experimental and calculated TG traces of the 50/40/10 EVA/ST/H12 blend and its pure components.

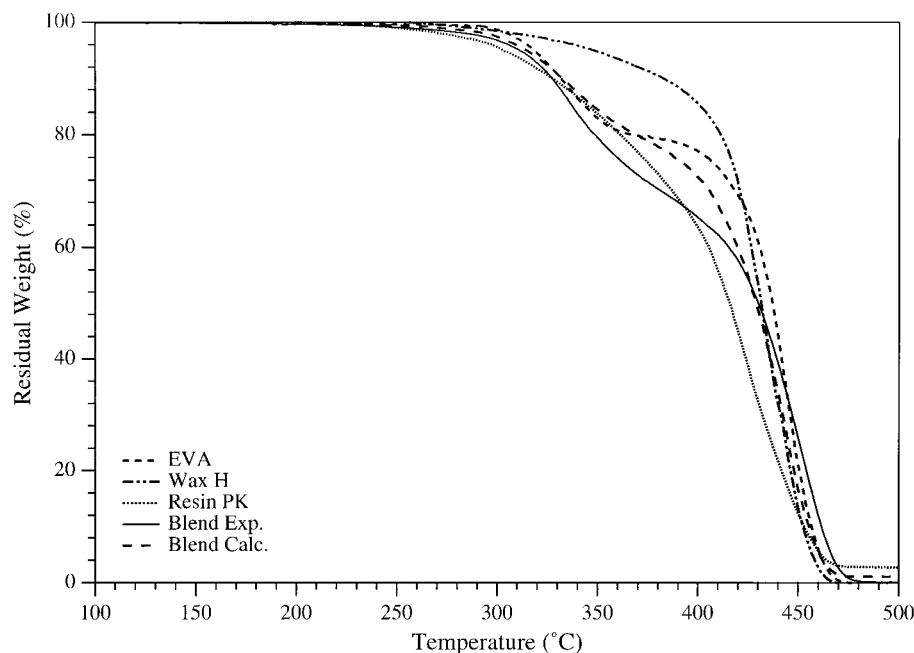


**Figure 3** Experimental and calculated TG traces of the 50/40/10 EVA/PK/H12 blend and its pure components.

the calculated trace (Fig. 2). However, above 320°C weight loss occurred more quickly than expected on the basis of the calculated trace. The apparent initial synergistic effect can be attributed to two concurrent processes implying a diffusion control of the degradation products of the ST resin as exerted by the more stable and viscous components (copolymer and wax) and interactions of the reactive species formed from the ST resin with EVA or H12. These should be able to modify their degradation mechanisms whose acceleration began to be detected at about 320°C. On the other hand, although the PK resin was more stable than the ST resin, the experimental trace of the EVA/PK/H12 blend (Fig. 3) began at a slightly lower temperature as indicated by the calculated trace. An interpretation for these observations can be made on the basis of the degree of resin dispersion into the polymer matrix. This could be in keeping with the fact that the PK resin could be more dispersed into the EVA and/or wax so that the diffusion of its decomposing species (small molecules or small radicals) through the more stable components would be more efficient, thus overwhelming its antagonist effect.

Table III presents decomposition temperatures based on two different definitions:  $T_d$  represents the temperature of a 1% weight loss deviation from the baseline<sup>17</sup> and  $T_{on}$  is the onset decomposition temperature corresponding to the temper-

ature taken in the correspondence of the crossover of tangents drawn on both sides of the decomposition trace.

The terpenic ST resin and the phenolic terpenic PK resin were the least stable blend components as previously pointed out. Their  $T_d$  values were 157 and 244°C, respectively, which were about 130°C lower than their onset temperatures. The difference between the  $T_d$  and  $T_{on}$  temperatures was related to the tangent angle from the onset definition and reflected the rate of the decomposition reaction. Therefore, this difference is larger for faster reactions. Taking into account this characteristic, the  $T_d$  was preferred for the ensuing discussion on material thermal decomposition.

The EVA/wax binary blends were more stable than their pure components; however, the EVA/resin/wax ternary blends were less stable than pure EVA. Blends containing the phenolic ST were characterized by  $T_d$  values of 270°C (EVA/PK/PE) and 261°C (EVA/PK/H12). These blends were about 30°C more stable than the corresponding formulations containing the ST terpenic resin.

In addition to the EVA-resin interactions as previously analyzed, it seemed very likely that there were other possible interactions between the degradation products of resin and wax that could further contribute to the blend decomposition process. Indeed, the  $T_d$  values of both EVA/



**Table III** Thermodegradation Temperatures of Evatane and Lotader Copolymers and Corresponding Three-Component Blends

Sample	$T_d$ (°C)	$T_{on}$ (°C)	Sample	$T_d$ (°C)	$T_{on}$ (°C)
EVA	291	307	AX	359	405
PE520	298	430	H12	232	403
PK500	244	372	ST5040	157	289
EVAPE	301	310	AXPE	355	409
EVAH	300	300	AXH	363	411
EVA2PKPE	270	300	AX2PKPE	247	403
EVA2PKH	261	306	AX2PKH	261	400
EVA2STPE	236	300	AX2STPE	233	295
EVA2STH	232	301	AX2STH	234	309

EVA and AX, Evatane and Lotader polymeric matrices, respectively; 2ST and 2PK, 40 wt % content of resins ST5040 and PK500, respectively; H and PE, 10 wt % content of waxes H12 and PE520, respectively;  $T_d$ , decomposition temperature at 1 wt % weight loss;  $T_{on}$ , onset decomposition temperature.

wax binary blends were almost equal to 300°C, even though the PE wax was 66°C more stable than the H12 wax. In the EVA/H12 blends the rise in  $T_d$  could be due to hydrogen bond interactions between the polar groups of the wax and acetate moieties of EVA. On the other hand, the results indicated that there were no interactions between the EVA and PE wax because the single components and the respective blend showed equivalent  $T_d$ 's. However, the H12 ternary blends were less stable than the corresponding PE formulations, this difference being more remarkable in the presence of the phenolic terpenic PK resin. By considering that several possibilities of reaction processes existed because of the combination of blend components and reactive species formed during thermal degradation, further investigations with complementary analytical methods are needed for a better understanding of the factors responsible for the decomposition and their relationship with blend performance.

### AX Blends

Experimental TG traces of AX/resin/H12 blends and their pure components are reported in Figures 4 and 5 in comparison with blend calculated traces. The AX/resin/PE blends exhibited similar TG profiles.

The AX blends behaved quite differently from the corresponding EVA blends. Indeed, all blend components decomposed in a single step but the ternary blend decomposition took place in two steps, at least in the investigated composition range. The thermal decomposition of the AX/ST/H12 blend occurred at a higher temperature than

that expected from the stability of its components (Fig. 4). A slight positive effect was also observed for the AX/PK/H12 blends (Fig. 5). Besides, the  $T_d$  values of the ternary blends (Table III) showed a more positive contribution by the H12 wax than by the PE wax. This synergistic effect may have been a consequence of AX interactions with the polar H12 wax. AX is an acrylic terpolymer that contains a glycidyl functional group that can react with acidic groups giving rise to covalent crosslinking bonds that are certainly 1 order of magnitude more stable than intermolecular hydrogen bonding interactions. In accordance, the  $T_d$  values of AX/H12 and AX/PE binary blends were 4°C higher and lower, respectively, than that of pure AX. The resin effect in AX ternary blends was similar to that observed in the EVA systems. This meant that blends containing the ST resin showed an apparent higher synergism. In contrast to the above results obtained for the last blends, the AX–H12 interactions had an additional role in the stability difference among blends with different resins. The  $T_d$  values of 247 and 261°C were found for AX/PK/PE and AX/PK/H12, respectively. However, corresponding blends containing ST resin presented  $T_d$  values 14 and 27°C lower, respectively. As already pointed out for EVA/resin/wax blends, further investigations are needed in order to get a better understanding of the factors responsible for the relative contributions to the decomposition of ternary blends.

### DSC of Different HMA Formulations

The EVA and AX blends were also investigated by DSC analysis. Representative DSC traces of EVA/

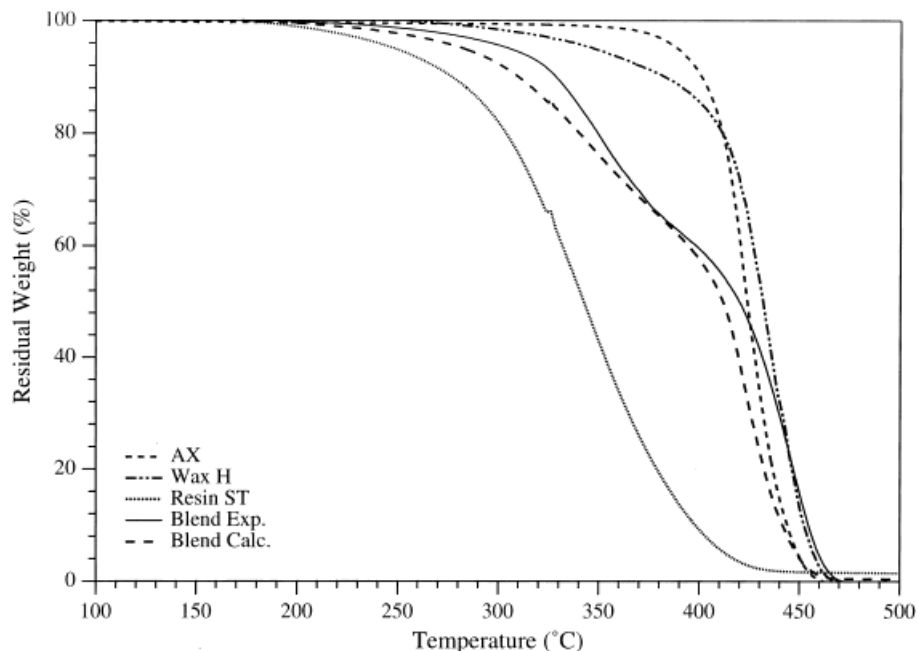


**Figure 4** Experimental and calculated TG traces of the 50/40/10 AX/ST/H12 blend and its pure components.

resin/wax and AX/resin/wax blends and their components recorded in the second heating cycle are reported in Figures 6 and 7. The polymeric matrices and waxes presented two overlapping melting peaks whereas the resin components did

not show any endothermic transition. The ternary blends exhibited two broad peaks whose positions roughly corresponded to those of the crystalline blend components. The intensity of these transitions was lower than that observed for the

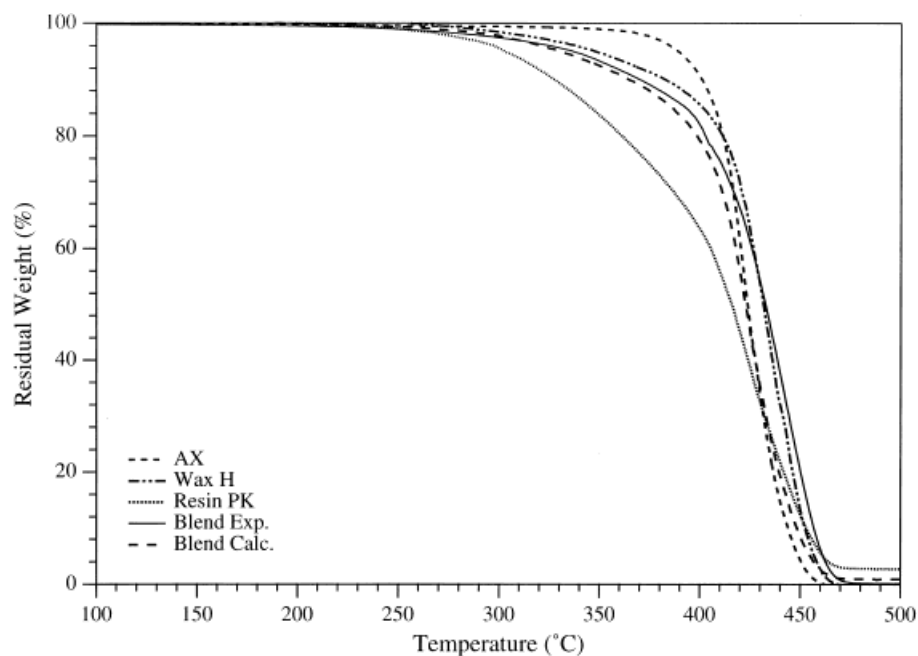


**Figure 5** Experimental and calculated TG traces of the 50/40/10 AX/PK/H12 blend and its pure components.

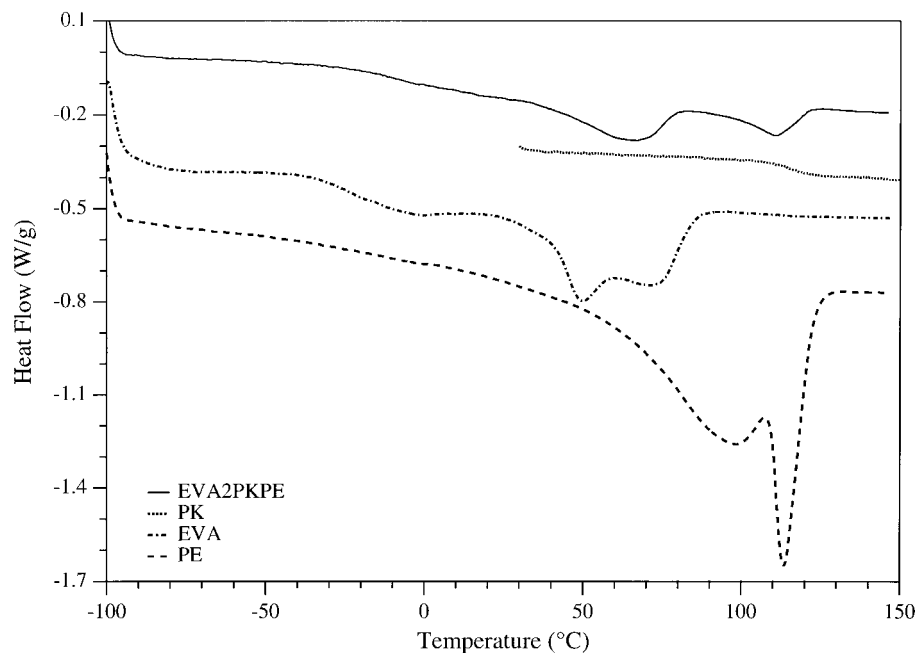


**Figure 6** DSC traces of the 50/40/10 EVA/PK/PE blend and its pure components.

individual blend components. Only in the EVA/resin/H12 blends (traces not shown) did the wax melting transition appear as a shoulder of the EVA melting peak. At a higher EVA concentration (70 wt %) this shoulder was less resolved and shifted at a lower temperature. This effect can be

attributed to the formation of less ordered H12 wax crystals due to "dilution" of the EVA and wax as a consequence of hydrogen bond interactions.

The thermodynamic parameters evaluated from DSC traces are listed in Tables IV and V, respectively. The  $\Delta T_p$  and  $\Delta T_w$  correspond to the

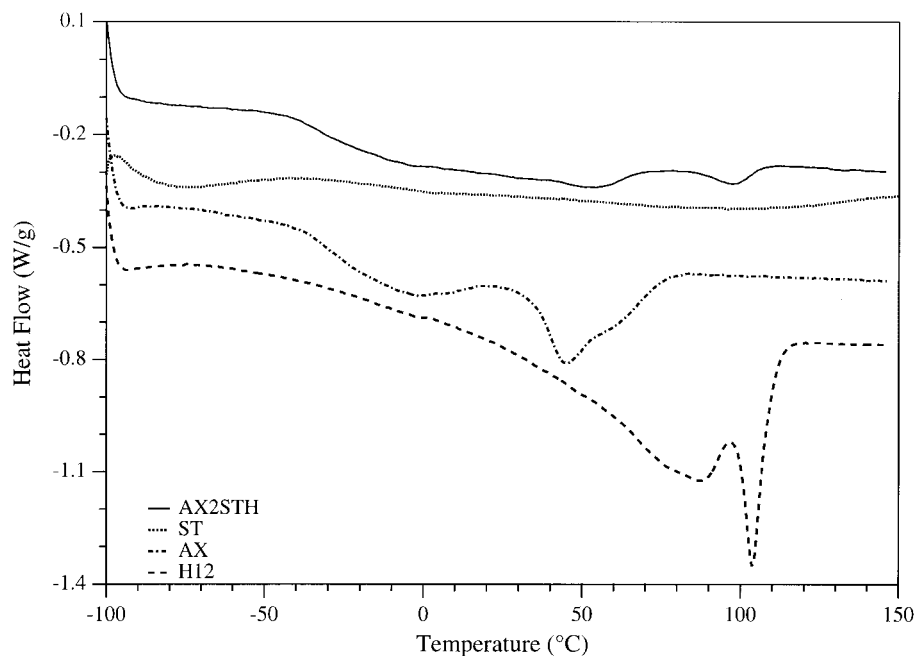


**Figure 7** DSC traces of the 50/40/10 AX/ST/PE blend and its pure components.



**Table IV** Thermodynamic Properties of Evatane Blends

Sample	$\Delta T_p$ (°C)	$T_{mp}$ (°C)	$\Delta H_{mp}$ (J g <sup>-1</sup> )	$\Delta T_w$ (°C)	$T_{mw}$ (°C)	$\Delta H_{mw}$ (J · g <sup>-1</sup> )
EVA <sup>a</sup>	80.7	50.2 70.2	32.2 26.8	—	—	—
H12 <sup>a</sup>	—	—	—	170.2	87.7 103.5	105.5 28.5
PE <sup>a</sup>	—	—	—	131.1	98.3 113.6	128.6 54.1
EVAH	113.2	70.3	59.2	ND	ND	ND
EVAPE	87.9	72.3	51.2	37.4	112.5	70.0
EVA <sup>a</sup> ST	86.4	64.3	50.0	—	—	—
EVA1STH	114.5	67.3	63.6	ND	ND	ND
EVA2STH <sup>a</sup>	112.3	64.3 86.4	62.0 10.4	ND	ND	ND
EVA1STPE	86.4	69.3	52.7	38.8	110.5	79.0
EVA2STPE	82.9	66.4	56.0	38.8	109.5	90.0
EVAPK	84.7	64.3	47.7	—	—	—
EVA1PKH	112.8	68.4	71.1	ND	ND	ND
EVA2PKH	115.9	66.4	78.8	ND	ND	ND
EVA1PKPE	87.8	70.4	62.6	39.2	112.5	93.0
EVA2PKPE	84.1	65.5	61.6	42.4	110.6	124.0

EVA, Evatane polymeric matrix; 1 and 2, 20 and 40 wt % resin concentrations, respectively; ST and PK, resins ST5040 and PK500, respectively; H and PE, waxes H12 and PE520 at 10 wt %, respectively;  $\Delta T_p$  and  $\Delta T_w$ , transition temperature ranges;  $T_{mp}$  and  $T_{mw}$ , melting peak temperatures;  $\Delta H_{mp}$  and  $\Delta H_{mw}$ , melting enthalpies of polymer and wax, respectively; ND, not determined due to the polymer melting tail.

<sup>a</sup> Overlapping peaks.

transition range;  $T_{mp}$  and  $T_{mw}$  are the melting peak temperatures; and  $\Delta H_{mp}$  and  $\Delta H_{mw}$  are the melting enthalpies of the polymer and wax, respectively. Enthalpies of overlapping peaks were evaluated from their estimated partial area.

The EVA blends exhibited a single  $T_{mp}$  at about 70°C, corresponding to the second overlapping melting transition of isolated EVA (Fig. 6). Moreover, the transition temperature range ( $\Delta T_p$ ) of EVA was increased, possibly due to the presence of closely spaced unresolved peaks.

The difference of the melting temperature of EVA and the first peak of the PE wax was about 10°C larger than that between EVA and H12. As a consequence, the DSC traces of EVA/resin/PE blends exhibited two well-separated melting transitions. All PE thermodynamic parameters decreased when going from the isolated wax to the ternary blend: the transition temperature range ( $\Delta T_w$ ) and  $\Delta H_{mw}$  decreased from about 130 to 40°C and from 183 to 90 J · g<sup>-1</sup>, respectively. Besides, the single melting peak temperatures, which were slightly lower than that of the second peak of the pure PE wax, decreased with the increase of the resin concentration.

Resins in binary blends bring about a slight decrease of the EVA peak temperature and en-

thalpy, indicating the establishment of a lower order in the phase organization. Similar behavior was reported by Komornicki et al.<sup>3</sup> for compatible EVA/terpene phenol resin binary blends. However, for ternary blends the enthalpy behaviors do not show any systematic trend. This can be attributed to the difficulty met in the determination of the true peak area corresponding to each phase due to partial overlapping of the transitions.

The difference of the melting temperatures of the AX and waxes allowed for a clear separation between their crystalline phase transitions with little overlapping. This reflected on the extension of the widening and narrowing of the transition temperature ranges of the AX and waxes, respectively. As mentioned above, the isolated AX polymer showed a melting peak with a maximum at 45°C and an overlapping shoulder at higher temperature (Fig. 7). However, DSC traces of the AX blends were characterized by the presence of a single AX melting peak with a maximum at 49–59°C, which corresponded to the peak shoulder of the parent polymer. This displacement of the melting peak temperatures toward the more ordered phase (high temperature side of the AX melting profile) suggested that resins and/or

**Table V** Thermodynamic Properties of Lotader Blends

Sample	$\Delta T_p$ (°C)	$T_{mp}$ (°C)	$\Delta H_{mp}$ (J · g <sup>-1</sup> )	$\Delta T_w$ (°C)	$T_{mw}$ (°C)	$\Delta H_{mw}$ (J · g <sup>-1</sup> )
AX	66.4	45.3	32.3	—	—	—
H12 <sup>a</sup>	—	—	—	170.2	87.7	105.5
PE <sup>a</sup>	—	—	—	131.1	103.5	28.5
					98.3	128.6
					113.6	54.1
AXH	81.5	59.4	23.0	ND	ND	ND
AXPE	80.7	57.4	22.3	42.7	116.5 <sup>b</sup>	26.0
AXST	72.7	50.4	22.3	—	—	—
AX1STH	78.0	53.4	22.3	37.0	100.5	37.0
AX2STH	77.1	54.3	25.6	35.2	97.4	48.0
AX1STPE	73.5	55.3	20.3	50.8	113.4 <sup>b</sup>	98.0
AX2STPE	72.2	52.5	24.8	52.1	109.5 <sup>b</sup>	102.0
AXPK	57.9	49.4	24.1	—	—	—
AX1PKH	84.7	52.5	35.1	35.2	99.6	40.0
AX2PKH	81.1	52.5	37.2	33.4	95.5	46.0
AX1PKPE	79.3	55.4	31.1	48.2	111.5	79.0
AX2PKPE	78.0	54.5	31.2	49.4	111.5	90.0

AX, Lotader polymeric matrix; 1 and 2, 20 and 40 wt % resin concentrations, respectively; ST and PK, resins ST5040 and PK500, respectively; H and PE, waxes H12 and PE520 at 10 wt %, respectively;  $\Delta T_p$  and  $\Delta T_w$ , transition temperature ranges;  $T_{mp}$  and  $T_{mw}$ , melting peak temperatures;  $\Delta H_{mp}$  and  $\Delta H_{mw}$ , melting enthalpies of polymer and wax, respectively.

<sup>a</sup> Overlapping peaks.

<sup>b</sup> Broad overlapping peak at lower temperature side.

waxes behave as nucleating agents on crystallization of the AX matrix.

The AX/H binary blends did not show any melting transition corresponding to the wax component. It can be supposed that the absence of the H12 wax crystalline phase is a consequence of crosslinking bonds, which are formed as indicated previously in the TG analysis. These interactions should occur in the less ordered portion of the AX crystalline phase. This interpretation was substantiated by the observed higher melting peak temperature (59.4°C) and lower enthalpy (23 J · g<sup>-1</sup>) of the AX/H12 blend with respect to the parent AX matrix (45.3°C and 32.3 J · g<sup>-1</sup>). On the contrary, in ternary blends the H12 wax tends to crystallize under the potential of the nucleating effect exerted by the resin on the wax and/or its control on crosslinking reactions between the AX matrix and H12 wax.

In AX/PE and AX/ST/PE blends the wax melting transition showed the two overlapped peaks characteristic of the parent PE wax. This similarity indicated crystalline phase separation and, consequently, incompatibility between the AX polymer and PE wax in the crystalline phase. However, in the AX/PK/PE blends a single peak for the wax phase was observed. This behavior can be explained by the lowering of the PE wax

enthalpy in these blends with a direct consequence on the detection of the shoulder at the lower temperature side.

As already indicated, the resins changed the crystal phase characteristics of the AX matrix and waxes. The influence on the peak temperature of the AX matrix did not present any particular trend with the resin concentration. This result suggested that competitive phenomena may have been occurring among the roles played by the wax and resin, thus tending to mask the individual effects, if any. On the other hand, we observed that the enthalpies of the crystalline phase of the AX and waxes were increased by increasing the resin concentration. However, it was observed that there was a higher difference in the wax enthalpies with the resin concentration when one of them was not polar (PE, ST) and the other was polar (H, PK). For example, the enthalpy difference for AX/ST/H was 11 J · g<sup>-1</sup> and for AX/ST/PE was 4 J · g<sup>-1</sup>. Thus, it can be reasonably assumed that there was a degree of nonpolar interactions in the PE-ST pair and hydrogen bond interactions for the H-PK pair that decreased the nucleation effect exerted by the resin with the increase of its concentration.

The  $T_g$ 's of both EVA and AX blends as taken from the inflection point in the DSC traces are

**Table VI Glass-Transition Temperature ( $T_g$ ) and Specific Heat ( $\Delta C_p$ ) as Function of Adhesive Composition**

Sample	$T_g$ (°C)	$\Delta C_p$ (J · g <sup>-1</sup> · K <sup>-1</sup> )	Sample	$T_g$ (°C)	$\Delta C_p$ (J · g <sup>-1</sup> · K <sup>-1</sup> )
EVA	-24.5	0.77	AX	-31.4	1.29
PK500	115.0	0.32	ST5040	49.3	0.16
EVAPE	-24.5	0.70	AXPE	-31.5	0.81
EVAH	-25.4	0.64	AXH	-30.5	0.91
EVA <sub>ST</sub>	-26.5	0.64	AX <sub>ST</sub>	-32.5	0.72
EVA1 <sub>STPE</sub>	-28.4	0.69	AX1 <sub>STPE</sub>	-32.5	0.97
EVA2 <sub>STPE</sub>	-31.4	0.61	AX2 <sub>STPE</sub>	-36.4	1.12
EVA1 <sub>STH</sub>	-26.5	0.87	AX1 <sub>STH</sub>	-33.5	0.95
EVA2 <sub>STH</sub>	-29.5	0.64	AX2 <sub>STH</sub>	-34.5	0.73
EVAPK	-5.5	0.24	AXPK	-6.5	0.30
EVA1 <sub>PKPE</sub>	-17.4	0.28	AX1 <sub>PKPE</sub>	-21.4	0.82
EVA2 <sub>PKPE</sub>	-8.3	0.30	AX2 <sub>PKPE</sub>	-7.4	0.44
EVA1 <sub>PKH</sub>	-12.4	0.60	AX1 <sub>PKH</sub>	-19.4	0.45
EVA2 <sub>PKH</sub>	-5.4	0.25	AX2 <sub>PKH</sub>	-9.4	0.33

reported in Table VI with the respective specific heats. All blends showed only one  $T_g$ . Because the resin  $T_g$ 's occurred in the same range of melting temperatures as the other two components, it was practically impossible to evaluate with the DSC technique whether they were present or not in the blends.

The  $T_g$  values of the polymer matrix/wax binary blends did not show a considerable difference from their analogous basic polymeric components. This indicated that the wax was not compatible with any polymer matrices in the amorphous phase. By contrast, in polymer matrix/resin binary blends a different behavior was observed. A slight decrease of the polymer matrix  $T_g$  was detected in both blends based on EVA and AX containing ST resin. The  $T_g$  values predicted by the simple Fox equation should have been -0.7 and -1.1°C for compatible EVA/ST and AX/ST blends, respectively. Consequently, the observed  $T_g$  decrease on these binary blends could be attributed to a decrease of the degree of crystallinity, although it was not possible to exactly define the enthalpies changes in the blends due to overlapped transitions. The same considerations could be drawn for the ternary blends. However, it was observed for polymer matrix/ST/wax blends that increasing the ST resin content decreased the blends'  $T_g$  more substantially in the formulations containing PE wax. The change in the crystalline phase of the matrix was not the only cause of change in the amorphous phase. A decrease of the  $T_g$  with blend composition can be a consequence of a plasticizing effect.<sup>13</sup> It can be supposed

that, because the ST resin and PE wax are both apolar, some compatibility effects are possible between them. As a consequence, the  $T_g$  of the resin decreases (not detected in ternary blends as already pointed out) and promotes higher mobility of the polymer matrices segments.

The polymer matrix/PK resin blend  $T_g$ 's were higher than the values observed for parent matrix polymers. The experimental values were -5.5 and -6.5°C for EVA/PK and AX/PK blends, respectively. These values were fairly close to the values predictable from the Fox equation (i.e., -0.5 and -0.7°C, respectively, for compatible blends). These results indicated that both polymer matrices were substantially compatible with the PK phenolic terpenic resin. Besides, ternary blends with the PK resin displayed an increase in the  $T_g$  with the increase of the resin content, as expected.

### Shear Strength of Adhesive

The adhesive performance measured by the shear strength of the EVA/resin/wax and AX/resin/wax blends in leather-rubber adherends are displayed in Table VII. The reported data are average values obtained from data collected on three samples, as measured at ambient temperature. Samples failed in a mixed mode where 70–90% of sample failure appeared to be cohesive in character with failure occurring within the bulk of the adhesive.

Adhesive shear strengths values presented little difference among EVA/wax binary blends.

**Table VII** Apparent Shear Strength of Adhesively Bonded Leather–Rubber Specimens

Sample	Apparent Shear Strength (MPa)
EVAH	0.830
EVAPE	0.826
EVA2STH	0.735
EVA2STPE	0.708
EVA2PKH	1.245
EVA2PKPE	1.208
AXH	0.918
AXPE	0.822
AX2PKH	1.070
AX2PKPE	1.180

However, in AX/wax binary blends the H12 polar wax showed a slightly superior performance with a value of 0.918 MPa.

Better results were obtained for EVA/PK/wax blends with values of shear strength at around 1.2 MPa. Turreda et al.<sup>11</sup> concluded that EVA/terpene phenol blends were miscible and that this property was directly related to the adhesive performance. So, it can be claimed that the performance obtained for both blends containing PK resin was due to hydrogen bond interactions of

this resin with the polymers matrices as already pointed out.

The ST terpenic resin presented the more negative effect on leather–rubber adhesion, showing lower values for EVA blends and no measurable values for AX/ST/wax blends due to film heterogeneity and extremely poor adhesion.

Figure 8 shows the apparent adhesive shear strength and  $T_g$  as a function of the adhesive formulation. We observed a direct relationship between the two properties.

Adhesion is a highly complex phenomenon involving the concepts of interfacial thermodynamics, interfacial rheology, and fracture mechanics. However, with the few results presented in Figure 8, it was possible in a simple way to correlate the two measured characteristics. Adhesive compositions containing ST terpenic resins were indicated to be incompatible systems. This means that there was poor interface interaction and basically no change in the  $T_g$  of each phase. When these materials are under shear loading, matrices as a elastic solid slip more easily than the resin ST glass solid. This inhomogeneity can give rise to voids as failure sites' propagation that is easier to initiate with a consequent decrease in the mechanical performance of the adhesive. On the

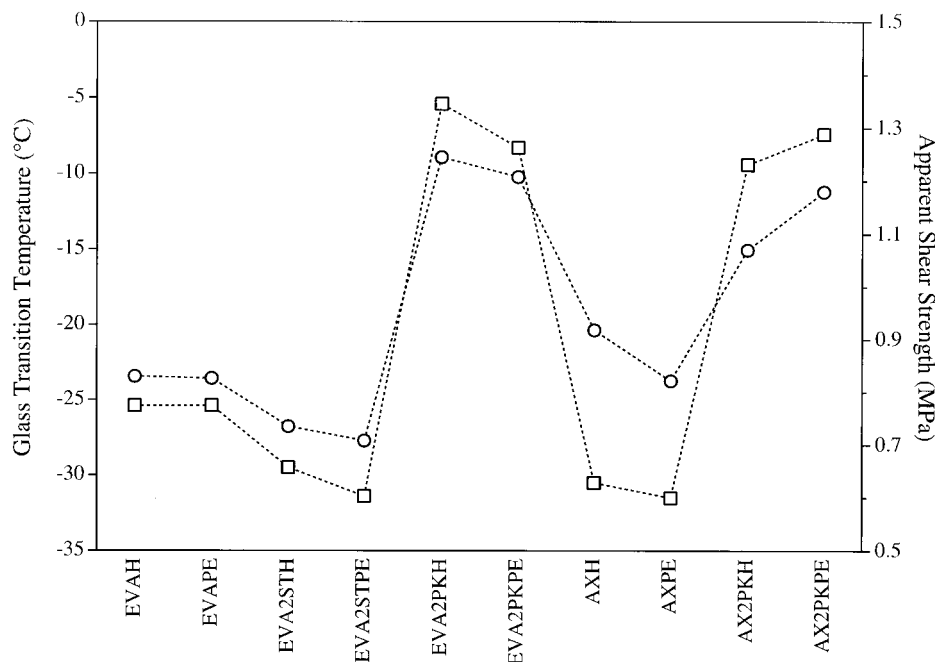


**Figure 8** The adhesive formulation dependence of the (□) glass-transition temperature of the adhesive systems and (○) apparent shear strength of adhesively bonded leather–rubber specimens.

other hand, the compatible adhesive formulations containing PK terpene phenolic resin with higher glass transition and intermolecular interactions result in a substantial configurational entropy decrease. This effect reflects on the decreasing of slipping of materials when a shear stress is applied. As a result, the adhesive material presents higher shear strength.

## CONCLUSIONS

Adhesive formulations for the footwear industry derived from three components (Evatane/resin/wax and Lotader/resin/wax blends) were studied as a function of the nature and concentration of the tackifier resin and the nature of the wax.

The EVA/resin/wax ternary blends were less stable than pure EVA. The lowering of its stability could be attributed to changes in the reaction mechanism due to the evolution of decomposition products of the less stable resin component. On the other hand, AX/resin/PE blends behaved differently, thus showing a synergistic effect as suggested by a comparison of experimental and simulated traces.

Basically, the EVA/resin/wax and AX/resin/wax ternary blends both showed equivalent results. Blend formulations containing ST terpenic resin resulted in incompatibility and lower adhesive performance. Different results were obtained for ternary blends containing PK terpene phenolic resin. A higher adhesive shear strength was recorded in agreement with their compatibility as ascertained by DSC measurements.

## REFERENCES

1. Lee, D. H.; Park, I. G.; Kim, J. H.; Lee, Y. H.; Kim, D.; Kang, S. K. *Neurotoxicol Teratol* 1998, 20, 259.
2. Fu, H.; Demers, P. A.; Costantini, A. S.; Winter, P.; Colin, D.; Kogevinas, M.; Boffetta, P. *Occupat Environ Med* 1996, 53, 394.
3. Komornicki, J.; Bourrel, M.; Marin, G.; Brogly, M. *J Adhes Sci Technol* 1992, 6, 293.
4. Shih, H.-H.; Hamed, G. R. *J Appl Polym Sci* 1997, 63, 323.
5. Shih, H.-H.; Hamed, G. R. *J Appl Polym Sci* 1997, 63, 333.
6. Honiball, W. J.; Lebez, J.; Simons, J. C.; van Rijn, K. *TAPPI J* 1997, 80, 179.
7. Galán, C.; Sierra, C. A.; Gómez Fatou, J. M.; Delgado, J. A. *J Appl Polym Sci* 1996, 62, 1263.
8. Sung, I. K.; Kim, K.-S.; Chin, I.-J. *Polym J* 1998, 30, 181.
9. Fujita, M.; Kajiyama, M.; Takemura, A.; Ono, H.; Mizumachi, H.; Hayashi, S. *J Appl Polym Sci* 1998, 70, 771.
10. Fujita, M.; Kajiyama, M.; Takemura, A.; Ono, H.; Mizumachi, H.; Hayashi, S. *J Appl Polym Sci* 1998, 70, 777.
11. Turreda, L. D.; Sekiguchi, Y.; Takemoto, M.; Kajiyama, M.; Hatano, Y.; Mizumachi, H. *J Appl Polym Sci* 1998, 70, 409.
12. Hale, A.; Bair, H. E. In *Thermal Characterization of Polymeric Materials*; Turi, E. A., Ed.; Academic: San Diego, CA, 1997; Chap. 4.
13. Bair, H. E. In *Thermal Characterization of Polymeric Materials*; Turi, E. A., Ed.; Academic: San Diego, CA, 1997; Chap. 10.
14. La Mantia, F. P. In *Handbook of Polymer Degradation*; Hamid, S. H., Amin, M. B., Maadhah, A. G., Eds.; Marcel Dekker: New York, 1992; p 95.
15. *Annual Book of ASTM Standards*, 15.06; American Society for Testing and Materials: Philadelphia, PA, 1993; p 199.
16. Dodson, B.; McNeill, I. C. *J Polym Sci Polym Chem Ed* 1976, 14, 353.
17. Fernandes, E. G.; Giolito, I.; Chiellini, E. *Thermochim Acta* 1994, 235, 67.